INFECTION AND IMMUNITY, Sept. 2005, p. 6110–6118 Vol. 73, No. 9
0019-9567/05/$08.00+0 doi:10.1128/IAI.73.9.6110–6118.2005

Anamnestic Responses of Mice following *Mycobacterium tuberculosis* Infection

Arati B. Kamath and Samuel M. Behar*

Division of Rheumatology, Immunology, and Allergy, Brigham and Women's Hospital and Harvard Medical School, Boston, Massachusetts 02115

Received 21 December 2004/Returned for modification 8 February 2005/Accepted 16 May 2005

The anamnestic response is the property of the immune system that makes vaccine development possible. Although the development of a vaccine against *Mycobacterium tuberculosis* is an important global priority, there are many gaps in our understanding of how immunological memory develops following *M. tuberculosis* infection or after BCG vaccination. In experiments designed to compare the anamnestic response of susceptible and resistant mouse strains, major histocompatibility complex-matched memory-immune C3.SW-H2^b/SnJ and C57BL/6 mice both demonstrated better control of bacterial replication following reinfection with *M. tuberculosis* than control mice. Nevertheless, this memory response did not appear to have any long-term protective effect for either mouse strain. A greater understanding of the immunological factors that govern the maintenance of immunological memory following exposure to *M. tuberculosis* will be required to develop an effective vaccine.

Mycobacterium tuberculosis is a major cause of morbidity and mortality in most regions of the world. Although tuberculosis has been a treatable disease for the last 50 years, the lack of an efficacious vaccine, poor access to healthcare, and the emergence and spread of drug-resistant *M. tuberculosis* are contributing to the reemergence of a global epidemic of tuberculosis (31). Consequently, the development of a vaccine that protects people against pulmonary tuberculosis is an international priority. Studies in people and in experimental animal models have shown that T-cell-mediated immunity is critical to control primary *M. tuberculosis* infection and to prevent the development of reactivation disease (6). Based on these principles, great emphasis is placed on immunization strategies that elicit mycobacterium-specific T cells (11). The development of a T-cell-based vaccine requires a thorough knowledge of how T-cell memory develops following vaccination (11). One of the greatest deficits in our knowledge is how the memory-immune response is affected by chronic infection. Advances in understanding the cellular basis for T-cell memory in other model systems have framed several questions that are relevant to how T-cell memory is generated following BCG vaccination or *M. tuberculosis* infection. These include understanding whether central or effector memory T cells protect the host from *M. tuberculosis*, whether the location of mycobacterium-specific memory T cells affects resistance, and how persistence of viable bacteria affects the development of memory T cells (13, 20, 27, 34).

Our original interest in these questions was to understand whether the susceptibility of certain inbred mouse strains arose from defects in T-cell function. For example, B6 mice survive longer than C3H mice following both IV and aerosol infection (3, 9, 10, 14). Contrary to our expectations, we found that the mycobacterium-specific T-cell response of susceptible C3H and resistant B6 mice was similar in many respects, particularly when major histocompatibility complex differences were taken into account (3, 9, 10). In fact, experiments using *M. tuberculosis*-infected, major histocompatibility complex-congenic mice showed that H-2^b-restricted T cells produced more gamma interferon (IFN-γ) when stimulated in vitro than H-2^k-restricted T cells. In contrast, for mouse strains with the same H-2 haplotype, T cells from infected C3H mice responded more robustly in vitro than T cells from mice of the B6 or B10 background (10). Consequently, the response of T cells from infected C3.SW-H2^b/SnJ mice is significantly greater than that of C3H/SnJ mice or B6 mice. Nevertheless, C3.SW-H2^b/SnJ mice are similarly susceptible as C3H/SnJ mice. However, immunological correlates of protective immunity are not well defined; therefore, there is concern whether the available assays used to detect alterations in T-cell phenotype or T-cell recognition of antigen can adequately assess differences in susceptibility. To address this problem from a functional perspective, we reasoned that the development of T-cell memory was a good measure of global T-cell function. Therefore, we sought to determine whether memory-immune B6 and C3H mice differed in their ability to control bacterial replication following rechallenge with *M. tuberculosis*.

The strategy we pursued was to cure *M. tuberculosis*-infected mice with antibiotics to generate memory-immune mice (12). The ability of these memory-immune mice, as well as previously naïve control mice, to control bacterial replication following challenge with *M. tuberculosis* was determined. Our results show that the memory-immune response provides enhanced protection, as measured by a more rapid control of bacterial replication early after infection. However, there was little long-term benefit when the survival of memory-immune and control mice was monitored. These results raise important questions concerning the development of immunity during my-

* Corresponding author. Mailing address: Division of Rheumatology, Immunology and Allergy, Brigham and Women's Hospital, Smith Building Room 516C, One Jimmy Fund Way, Boston, MA 02115. Phone: (617) 525-1033. Fax: (617) 525-1010. E-mail: sbehar@rics.bwh.harvard.edu.

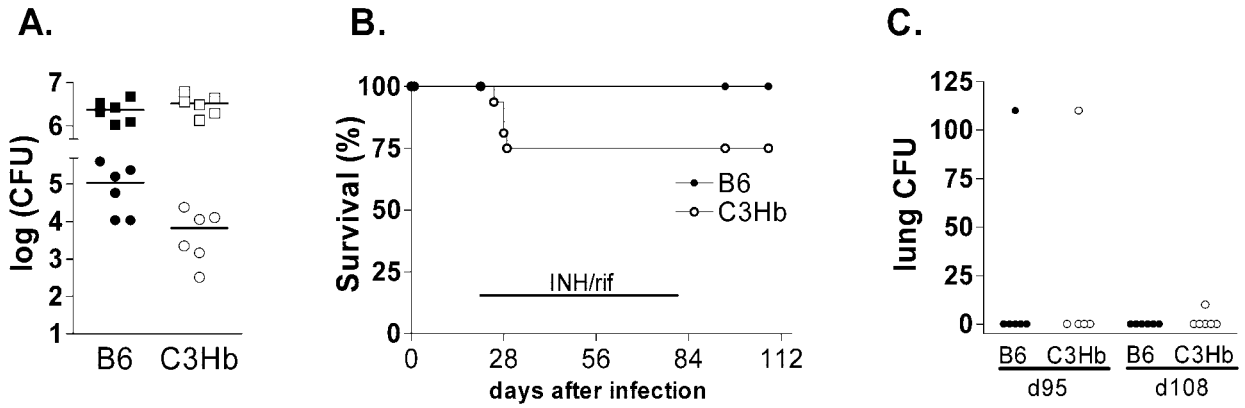

FIG. 1. Generation of memory-immune mice. (A) Bacterial burden in the lungs and spleens of B6 and C3.SW-H2^b/SnJ mice following primary infection. The number of bacteria in the lungs (squares) and spleens (circles) of B6 (closed symbols) and C3.SW-H2^b/SnJ (C3Hb) (open symbols) mice was determined 21 days after primary infection with *M. tuberculosis* by the aerosol route. Six mice per group were used, and the results show the CFU from each individual mouse. The bars represent the medians. (B) The survival of B6 and C3.SW-H2^b/SnJ (C3Hb) mice following primary *M. tuberculosis* infection. Starting on day 21, mice were treated with isoniazid (INH) and rifabutin (rif) for 60 days. The bars indicate the treatment periods. (C) The bacterial burden in the lungs of antibiotic-treated mice. The lung CFU of B6 (closed circles) and C3.SW-H2^b/SnJ (C3Hb) (open circles) mice was determined on days 95 (d95) and 108 (d108) after primary infection (14 and 27 days after the cessation of antibiotic treatment). Six mice per group were used, and the CFU from individual mice is plotted on a linear scale. The limit of detection is 10 CFU/mouse lung.

cobacterial infection, the role of bacterial persistence, and the long-term function of T cells during chronic inflammation.

MATERIALS AND METHODS

Mice. A cohort of 136 age-matched female C57BL/6 (B6) and C3.SW-H2^b/SnJ mice was obtained from Jackson Laboratories (Bar Harbor, ME). Mice were housed in a biosafety level 3 facility under specific-pathogen-free conditions at the Animal Biohazard Containment Suite (Dana Farber Cancer Institute, Boston, MA) and were used in a protocol approved by the institution.

Bacteria and aerosol infection. Virulent *M. tuberculosis* (Erdman strain) cells were prepared as previously described (2). Forty-eight mice of each strain were infected via the aerosol route using a nose-only exposure unit (Intox Products, Albuquerque, NM) (2). A second infection was done using 50 memory-immune mice (28 C3.SW-H2^b/SnJ and 22 B6 mice from the first infection) and 40 additional uninfected control mice (20 of each strain) that were from the original cohort of mice. All time points used six mice/group.

Antibiotic treatment. Between days 21 and 81, isoniazid and rifabutin (both at 100 mg/liter) were added to the drinking water of infected mice. The drinking water was changed twice weekly during the treatment period, and the mice had access to the water ad libitum.

CFU determination. After euthanasia by CO_2 inhalation, the inferior vena cava was severed and blood was purged from the lungs by perfusing with RPMI 1640 through the right ventricle of the heart. The left lung and half a spleen were aseptically removed and individually homogenized in 0.9% NaCl–0.02% Tween 80 with Mini-Bead Beater 8 (Biospec Products, Bartlesville, OK). CFU were quantified by plating 10-fold serial dilutions of organ homogenates onto 7H11 Mitchinson agar plates (Remel, Lenexa, Kansas). Colonies were counted after 3 weeks of incubation at 37°C.

Flow cytometry. Splenocytes were prepared by standard protocols, and lung mononuclear cells (MNC) were prepared by collagenase digestion of lung tissue after intravascular perfusion with phosphate-buffered saline as previously described (9, 10). One million splenocytes or lung MNC were stained with antibodies to CD4, CD8, CD11a, and CD69 or an appropriate isotype control (all from Pharmingen, San Diego, CA). After fixation with 1% paraformaldehyde and storage at 4°C overnight, the cells were analyzed using a FACSort (Becton Dickinson, San Jose, CA) flow cytometer. The FlowJo software program was used to analyze the data (Tree Star Inc., Stanford, CA).

In vitro restimulation assays. Lung MNC in vitro restimulation assays were done as previously described (2, 9, 10). Lung mononuclear cells (3×10^6 cells/ml) in a volume of 2 ml were incubated in complete medium in the presence of *M. tuberculosis* H37Ra sonicate (11) (diluted 1:1,000, 1:5,000, or 1:25,000) or Ag85 (obtained from John Belisle, Colorado State University, through the National Institutes of Health/National Institute of Allergy and Infectious Diseases contract NO1-AI-75320 entitled "Tuberculosis Research Materials and Vaccine Testing") at 3.3 or 10 μg/ml or in medium alone for 48 h at 37°C. Culture supernatants were assayed for cytokines by an enzyme-linked immunosorbent assay by using antibody pairs and cytokines from Pharmingen (San Diego, CA).

BAL. Bronchoalveolar lavage (BAL) fluid was collected as previously described (9, 10). Briefly, the trachea was exposed and repeatedly lavaged four or five times with a single 1-ml aliquot of sterile 0.005 M EDTA in phosphate-buffered saline. The BAL fluid was stored at −80°C prior to its assay by cytokine enzyme-linked immunosorbent assay.

Histological analysis. Lung tissue was preserved in Z-fix (Anatech, Battle Creek, MI) and then embedded in paraffin. Five-μm-thick sections were stained with hematoxylin and eosin stain, trichrome stain, or acid-fast bacillus (AFB) staining to confirm the bacterial load in the lung (11). Images were obtained using a Leica DMLB microscope and a Nikon Coolpix 9500 digital camera. The images were adjusted and assembled in Adobe Photoshop 7.0.

Statistics. The Prism software program was used to perform all statistical analyses (Graphpad, San Diego, CA). CFU were $\log_{10}$ transformed before analysis. The statistical significance of two-way comparisons was tested using a two-tailed *t* test. The statistical significance of multiple CFU comparisons was tested using the nonparametric Kruskal-Wallis test with Dunn's posttest, which makes no assumptions about the normality of the data (i.e., it is a nonparametric test). Other multiple comparisons were performed using two-way analysis of variance using Bonferroni posttests. The log rank test using the Kaplan-Meier method was used to compare differences in the survival of mouse strains.

RESULTS

Generation of memory-immune mice. We have previously shown that C3H mice are more susceptible than B6 mice based on survival, both after intravenous and aerosol infection with virulent *M. tuberculosis* (3, 10). While the H-2 haplotype affects the T-cell recognition of mycobacterial antigens, susceptibility of C3H mice is independent of the H-2 haplotype (10).

Based on our previous work, susceptible C3.SW-H2^b/SnJ and resistant B6 mice were infected by the aerosol route with virulent *M. tuberculosis*. On day 20 after infection, six mice per strain were sacrificed and the CFU in the lung and spleen were enumerated. As expected, the bacterial burden in the lungs of B6 and C3.SW-H2^b/SnJ mice was similar (Fig. 1A) (2, 10). In contrast, fewer CFU were detected in the spleens of C3.SW-H2^b/SnJ mice than in B6 mice ($P = 0.0112$), which has been

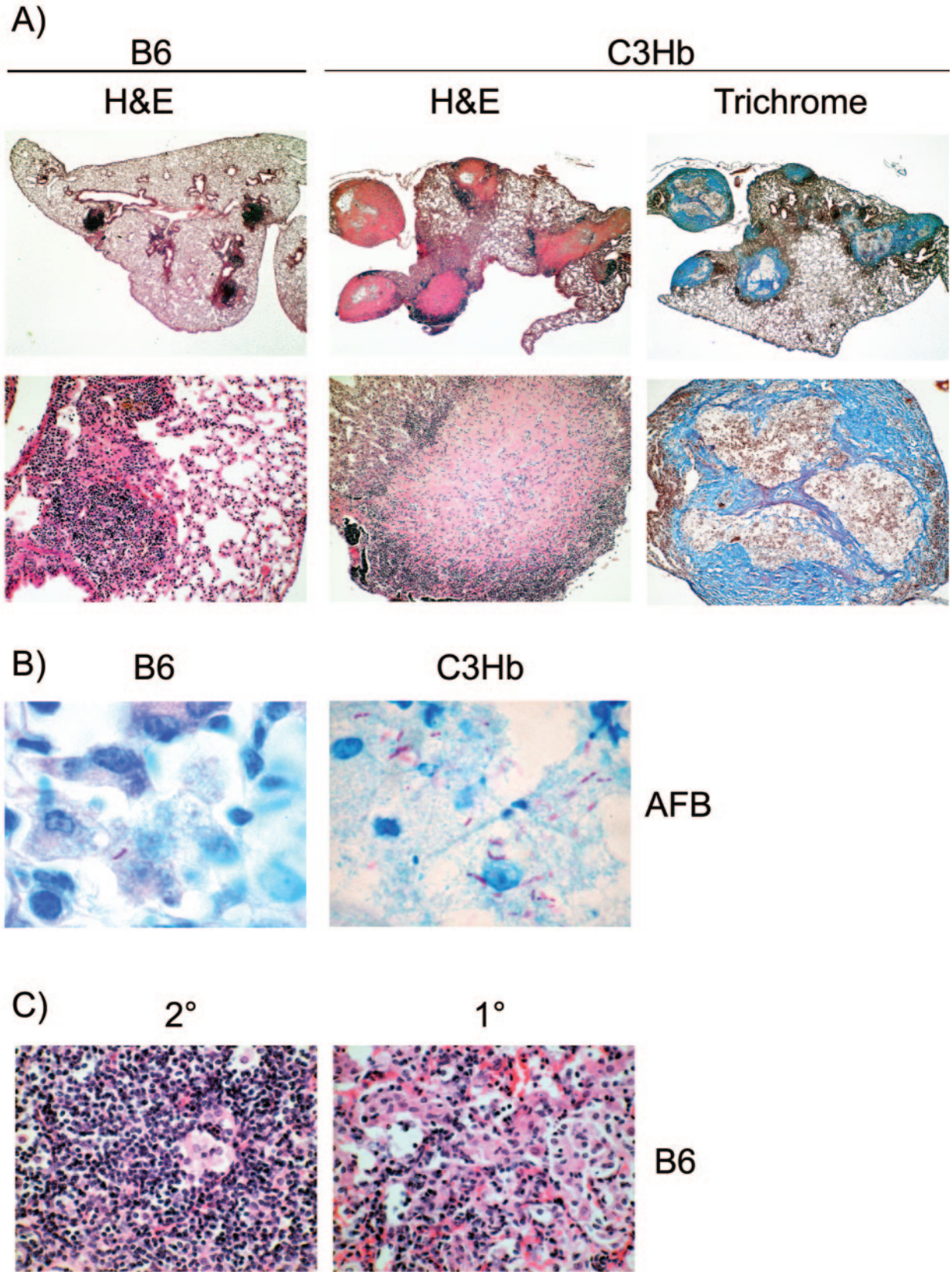

FIG. 2. Tissue histopathology of the lung in memory-immune mice. (A) *M. tuberculosis*-infected B6 and C3.SW-H2^b/SnJ (C3Hb) mice were sacrificed after receiving 60 days of antibiotic treatment followed by 30 days of rest. Representative lung sections are shown stained with hematoxylin and eosin (H&E) or trichrome stain. Magnifications: top row, ×25; bottom row, ×200 (B6) or ×100 (C3Hb). (B) Lung tissue from the B6 and C3.SW-H2^b/SnJ (C3Hb) mice depicted in panel A was stained for AFB. The photographs were from the periphery (B6) or center (C3Hb) of the granuloma. Magnification, ×1,000. (C) Representative histological appearance of granulomas 21 days after infection from B6 memory-immune mice (2°) or previously naïve mice (1°). Magnification, ×600.

TABLE 1. Summary of pathological findings of *M. tuberculosis*-infected mice

Immune status before challenge with *M. tuberculosis* and mouse strain	Summary of pathological findings
Previously naïve	
B6	Medium to large areas of granulomatous inflammation, especially in the peribronchial and perivascular areas, with some lymphocytes and scattered PMN; AFB present
C3.SW-H2^b/SnJ	Small to medium areas of granulomatous inflammation, especially in the peribronchial and perivascular areas, with some lymphocytes and scattered PMN; AFB present
Memory immune	
B6	Mostly small to medium, discrete granulomas with prominent lymphocytic infiltrates, some foamy macrophages, some with hemosiderin deposits; few AFB detected
C3.SW-H2^b/SnJ	Small to medium areas of granulomatous inflammation, some discrete granulomas with prominent lymphocytic infiltrates, foamy macrophages prominent, some with hemosiderin deposits; few AFB detected

previously reported to arise from delayed systemic bacterial dissemination in C3H mice compared to B6 mice (2, 10).

To make memory-immune mice, infected B6 and C3.SW-H2^b/SnJ mice were treated with isoniazid and rifabutin starting on day 21 for a total of 60 days. During the fourth week of infection, four C3.SW-H2^b/SnJ mice died but no other deaths occurred during the first phase of the experiment (Fig. 1B). On day 81, the antibiotics were discontinued and the mice were observed for another 30 days.

Groups of mice were sacrificed on day 95 and 108 to ascertain whether the antibiotic regimen successfully sterilized the lungs of infected mice. No CFU were detected in the lungs of 20 out of 23 mice analyzed (level of detection = 10 CFU). In three mice, between 10 and 110 CFU were detected (Fig. 1C). This degree of sterilization was similar to that reported by other studies examining the memory-immune response in antibiotic-treated mice (21, 29). On day 111 postinfection, the remaining mice (hereafter referred to as memory-immune mice) were challenged with *M. tuberculosis* by the aerosol route. In addition, age- and gender-matched mice from the same original cohort that had not been originally infected were infected at the same time (these control mice will be referred to as previously naïve mice). This design allowed us to simultaneously compare the primary and secondary responses in B6 and C3.SW-H2^b/SnJ mice.

Granuloma formation and T-cell activation in memory-immune mice. Following antibiotic treatment, we observed that the pulmonary granulomatous lesions underwent consolidation and became small, dense lesions made up predominantly of lymphocytes (for an example, see B6 lung in Fig. 2A). In a separate experiment of similar design during which full sterilization of the lungs was not achieved, the lesions of the C3.SW-H2^b/SnJ mice continued to evolve and more closely resembled human granulomas. For example, a rim of lymphocytes was clearly defined and the centers of the granulomas were somewhat necrotic, as indicated by the pale eosinophilic centers of the nodules, some which began to cavitate (Fig. 2A). The granuloma centers contained cellular debris and scattered polymorphonuclear and myeloid cells. The nodules were largely fibrotic, as can be observed by the extensive extracellular matrix stained blue by the trichrome stain (Fig. 2A). Acid-fast bacteria were detected in the lesions of both B6 and C3.SW-H2^b/SnJ mice. While the AFB in the B6 mice were detected within macrophages found in the periphery of the lesions, most of the bacteria in the C3.SW-H2^b/SnJ mice were detected in the centers of the necrotic granulomas (Fig. 2B). These findings contrast with the pathological picture in C3H mice following primary respiratory infection under standard conditions. One typically observes granulomatous inflammation without discrete granuloma formation and a paucity of lymphocytic infiltrates. Instead, one sees intense neutrophilic infiltrates and diffuse necrosis (9, 10). We hypothesize that because of the fulminate nature of this process in C3H mice, the lesions do not ordinarily have time to evolve. In this experiment, mice were rescued using antibiotics and consequently, the lesions had an opportunity to evolve and partially heal.

In contrast, the histopathologies of the lungs of B6 and C3.SW-H2^b/SnJ mice from the experiment depicted in Fig. 1C, in which the lungs were successfully sterilized, were similar to each other. The majority of the lung tissue appeared normal except for between zero and four small healing lesions with dense lymphocytic infiltrates, similar to the ones in the lungs of the B6 mice depicted in Fig. 2A. Granuloma formation after infection differed between memory-immune and previously naïve mice. When examined 21 days after rechallenge, the granulomas found in the lungs of memory-immune mice had more prominent lymphocytic infiltrates, which is likely to be a consequence of more rapid activation and recruitment of T cells into the lung (Fig. 2C and Table 1).

By day 21 after infection, previously naïve and memory-immune mice recruited similar numbers of T cells to the lung ($\sim 6 \times 10^6$ to 7×10^6/lung) and there was no difference between B6 and C3.SW-H2^b/SnJ mice (data not shown). Memory-immune mice had more pulmonary T-cell activation than previously naïve mice. The cell surface expression of CD11a, which is upregulated on antigen-experienced and memory T cells (26, 33), and of CD69, which is a T-cell activation marker (30), was measured 21 days after *M. tuberculosis* challenge. A greater percentage of CD11a^{HI} CD4$^+$ and CD8$^+$ T cells from the lungs of memory-immune mice expressed the activation marker CD69 (Fig. 3 and data not shown). For CD8$^+$ CD11a^{HI} T cells, 42.1% and 72.8% expressed CD69 in the lungs of memory-immune B6 and C3.SW-H2^b/SnJ mice, respectively, compared with 18.8% and 48.3% for the previously naive mice (Fig. 3). For the CD4$^+$ CD11a^{HI} T cells, 61.1% and 81.0%

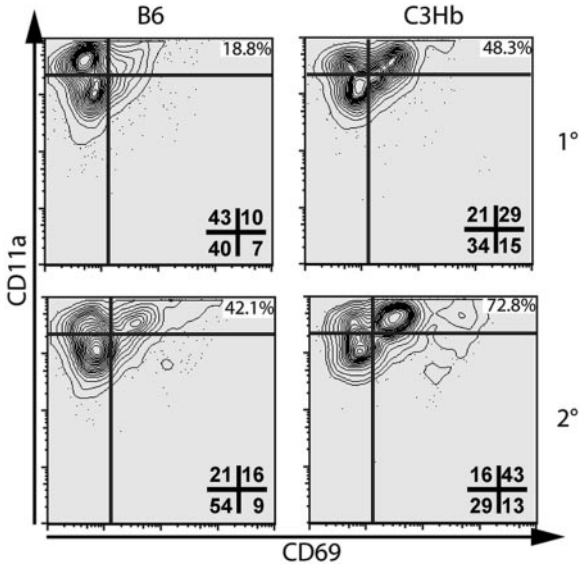

FIG. 3. Activation of pulmonary T cells following *M. tuberculosis* infection. $CD8^+$ T cells from the lungs of previously naïve (1°) or memory-immune (2°) B6 and C3.SW-$H2^b$/SnJ (C3Hb) mice were analyzed 21 days after infection for their expression of CD11a and CD69. While all $CD8^+$ T cells expressed CD11a, subpopulations that expressed high or intermediate levels could be identified. The percentage of $CD11a^{HI}$ cells expressing CD69 is shown. The percentage of cells in each quadrant is shown in the lower part of each plot.

expressed CD69 in the lungs of memory-immune B6 and C3.SW-$H2^b$/SnJ mice, respectively, compared with 34.9% and 65.4% for the previously naive mice (data not shown). We believe that these results may indicate that memory-immune mice have more efficient activation and/or expansion of memory T cells than previously naïve mice. The total percentage of $CD11a^{HI}$ cells is lower in the secondary B6 response than the primary B6 response, and this may be due to the kinetics of the response.

These results are consistent with the increased frequency of activated memory $CD4^+$ and $CD8^+$ T cells following secondary infection observed by others (30). We have also studied the expression of CD62L and CD45RB in the memory-immune and previously naïve mice following rechallenge and did not observe differences with these markers between the memory-immune and previously naïve mice or between B6 and C3.SW-$H2^b$/SnJ mice at the time points in this study (see reference 10 for modulation of CD69, CD11a, and CD62L during the primary immune response) (data not shown). In these experiments, we observed a uniform decrease in the expression of CD62L and CD45RB in all groups (data not shown), which is not surprising since these markers do not distinguish between activated and effector memory T cells.

We have previously shown that IFN-γ is detected in the BAL fluid of C3.SW-$H2^b$/SnJ mice following infection and correlates with their mycobacterial-antigen-specific T-cell immune response (10). Following sterilization with antibiotics, the amount of IFN-γ detected in the BAL fluid was decreased in both B6 and C3.SW-$H2^b$/SnJ mice (Fig. 4A). Increased IFN-γ levels were found in both previously naïve and memory-immune mice 21 days after infection with *M. tuberculosis* (Fig. 4A). Although similar levels were found in both B6 and C3.SW-$H2^b$/SnJ mice, increased levels were detected in the memory-immune mice, consistent with the greater T-cell activation and T-cell production of IFN-γ production as observed by others (30).

Although there was no difference in the BAL fluid levels of IFN-γ between B6 and C3.SW-$H2^b$/SnJ mice, we detected considerably more IFN-γ production by C3.SW-$H2^b$/SnJ lung MNC (Fig. 4B and C). A similar pattern was observed in the draining pulmonary lymph node and in the spleen (data not shown). This is consistent with our previous observation that T cells from C3.SW-$H2^b$/SnJ mice proliferate more and produce more IFN-γ than T cells from H-2^k mice or mice of the B6 or B10 background (10). A clear difference between the primary and secondary recall response in the lung was not observed, contrary to our expectations, which may have been due to the secondary response peaking earlier than the primary response (30). Interestingly, the secondary response of C3.SW-$H2^b$/SnJ mice differed qualitatively from the primary response. For the secondary response, the *M. tuberculosis* sonicate induced more IFN-γ, while Ag85 induced less IFN-γ, which may indicate a diversification of the immune response in C3.SW-$H2^b$/SnJ mice (Fig. 4C). We speculate that the overexuberant immune response of C3.SW-$H2^b$/SnJ mice could contribute to their increased susceptibility, although this is tempered by our find-

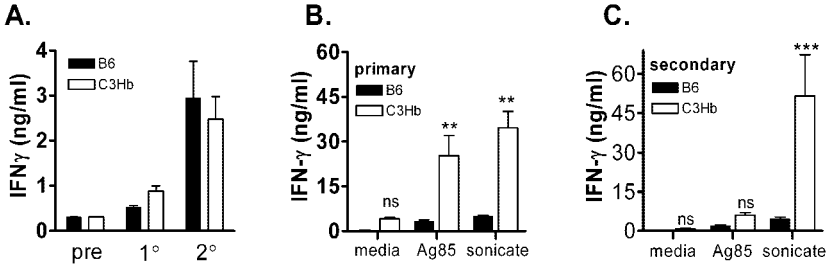

FIG. 4. Immunity following respiratory *M. tuberculosis* infection. (A) The concentration of IFN-γ in the BAL fluid was measured after treatment with antibiotics (pre) and 21 days after challenge of previously naïve mice (1°) or memory-immune mice (2°). Data represent the means of six mice per group plus standard error. (B) IFN-γ production by lung MNC isolated from previously naïve B6 and C3.SW-$H2^b$/SnJ mice 21 days after respiratory infection with *M. tuberculosis*. Lung MNC were cultured in vitro in media alone or stimulated with Ag85 (10 μg/ml) or *M. tuberculosis* sonicate (1:5,000 dilution). (C) IFN-γ production by lung MNC isolated from memory-immune B6 and C3.SW-$H2^b$/SnJ mice 21 days after respiratory infection with *M. tuberculosis* was performed as described for panel B. C3Hb, C3.SW-$H2^b$/SnJ. **, $P < 0.01$, and ***, $P < 0.001$, by two-way analysis of variance using Bonferroni's posttest.

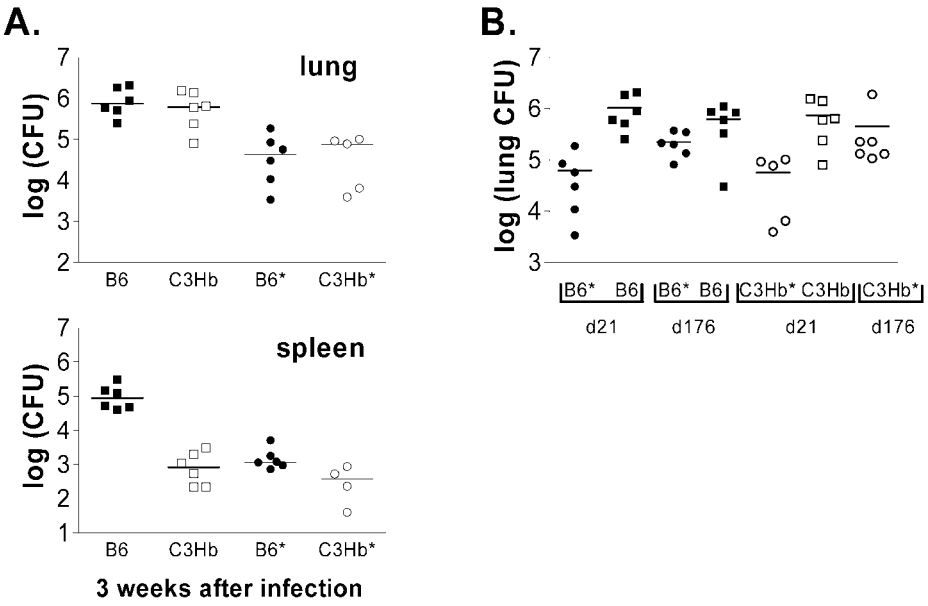

FIG. 5. Bacterial burden in the lungs and spleens of B6 and C3.SW-H2^b/SnJ mice after secondary infection. Age- and gender-matched previously naïve (squares) or memory-immune (circles) B6 (closed symbols) and C3.SW-H2^b/SnJ (C3Hb) (open symbols) mice were infected by the respiratory route with *M. tuberculosis*. Six mice per group were used, and each symbol represents the CFU results from an individual mouse. The bars represents the medians. *, memory immune. (A) The bacterial load was measured in the lungs and spleens 21 days after infection. (B) The lung bacterial burden 6 months after secondary infection. The results obtained on day 21 (d21) (from Fig. 5A) are repeated here for comparison.

ing that other substrains of C3H mice of the H-2^k haplotype make significantly less IFN-γ but are similarly susceptible (10).

The memory response more effectively controls bacterial replication. We assessed whether the memory-immune response could protect susceptible C3.SW-H2^b/SnJ mice similarly to resistant B6 mice. The ability of memory-immune B6 and C3.SW-H2^b/SnJ mice to control bacterial replication was compared to that of previously naïve B6 and C3.SW-H2^b/SnJ mice. Because the memory-immune response peaks more rapidly than the primary immune response (30), we hoped to detect a difference between previously naïve and memory-immune mice 3 weeks after rechallenge with *M. tuberculosis*. The lung bacterial burden was similar in previously naïve B6 and C3.SW-H2^b/SnJ mice (Fig. 5A). In contrast, the lung bacterial burden in memory-immune mice was nearly 1 log less than that in previously naïve mice ($P < 0.01$ and < 0.05 for B6 and C3.SW-H2^b/SnJ mice, respectively, by the Kruskal-Wallis test with Dunn's posttest). B6 and C3.SW-H2^b/SnJ memory-immune mice did not differ from each other (Fig. 5A). In an independent experiment, the lung CFU did not differ between memory-immune B6 and C3.SW-H2^b/SnJ mice. In the spleen, the protective effect of the memory-immune response was approximately 2 logs in B6 mice. The spleen bacterial burdens of B6 and C3.SW-H2^b/SnJ memory-immune mice and previously naïve C3.SW-H2^b/SnJ mice were similar. In contrast, previously naïve B6 mice had more bacteria in the spleen than the other groups ($P < 0.001$), which is likely to be a consequence of early dissemination, as discussed above (Fig. 1). Thus, by these standard measurements, both B6 and C3.SW-H2^b/SnJ mouse strains mount a protective memory-immune response.

Another time point was done on experimental day 287, 176 days after the mice were rechallenged with *M. tuberculosis* (Fig. 5B). For the previously naïve B6 mice, there was little difference in the lung bacterial burden between day 21 and day 176. In contrast, the lung bacterial burden increased in B6 memory-immune mice between day 21 and day 176. This plateau or chronic stable phase is typically observed and represents the attainment of equilibrium between bacterial replication and immune control. Sufficient numbers of previously naïve C3.SW-H2^b/SnJ mice were unavailable for the day 176 time point, as many had succumbed by this late time point; however, the lung CFU of C3.SW-H2^b/SnJ memory-immune mice increased from day 21 to day 176 postinfection, as was observed for B6 mice. Thus, while the lung CFU of the previously naïve mice remained relatively constant during the course of the experiment, the lung bacterial burden in memory-immune mice slowly increased between day 21 and day 176, although testing did not show these differences to be statistically significant. The observed convergence of pulmonary CFU 6 months after infection minimized the beneficial effect of the memory response.

The effect of the memory response on survival. To determine the long-term benefit of memory in host defense against tuberculosis, the survival of memory-immune mice was compared to that of previously naïve mice (Fig. 6). Because of the prolonged duration of this experiment, four uninfected age- and gender-matched mice of each strain were housed in parallel and survived more than 600 days (data not shown). Surprisingly, there was no difference in the survival of previously naïve and memory-immune C3.SW-H2^b/SnJ mice (mean survival time, 168 and 163, respectively). Memory-immune B6 mice survived longer than previously naïve B6 mice (401.5 days versus 343 days; $P = 0.027$), but it is uncertain whether this 17% increase in mean survival time is biologically significant.

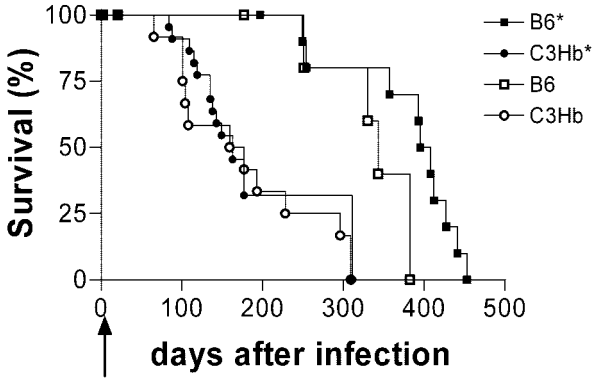

FIG. 6. Survival of previously naïve and memory-immune B6 and C3.SW-H2^b/SnJ mice following respiratory infection with *M. tuberculosis*. Age- and gender-matched control (open symbols) or memory-immune (closed symbols) B6 (squares) and C3.SW-H2^b/SnJ (C3Hb) (circles) mice were infected by the respiratory route with *M. tuberculosis* and their survival monitored. Numbers of days after the second aerosol infection are shown. The arrow corresponds to day 111 in Fig. 2. *, memory immune.

These data show that the enhanced protection observed in memory-immune mice 21 days after infection does not necessarily predict the long-term outcome of *M. tuberculosis* infection.

DISCUSSION

To better understand the memory-immune response in susceptible and resistant mouse strains, memory-immune mice were generated by sterilizing *M. tuberculosis*-infected mice with antibiotics. Following a rest period, both memory-immune and previously uninfected age-matched controls were infected with *M. tuberculosis* by the aerosol route. Three weeks after secondary infection, a memory-immune response was detected in both susceptible C3H and resistant B6, as indicated by the more effective control of bacterial replication than that in previously uninfected control mice. These results are consistent with other reports of enhanced bacterial control observed in mice previously infected with *M. tuberculosis* and then sterilized using antibiotics (4, 30). Despite evidence of a memory response, the mortality of memory-immune and naïve C3H mice was indistinguishable. Similarly, memory-immune B6 mice had only a modest increase in survival compared to previously naïve B6 mice.

Why mice ultimately die from tuberculosis is not well understood, although it is related to the total bacterial load and immunopathology. During the acute phase of respiratory *M. tuberculosis* infection, the immune system controls bacterial replication within 2 to 4 weeks. The lung bacterial burden then remains stable in a plateau or stationary phase following both IV and respiratory infection (22, 32). Late during infection, recrudescence can occur, as signified by increased bacterial replication in the lung, which often precedes death. Why recrudescence occurs is poorly understood. Orme showed that T cells taken from mice during the recrudescence phase of disease were still able to transfer resistance to control mice (22). This paradox, that T cells unable to control bacterial replication in chronically infected mice could provide protection to naive mice from *M. tuberculosis*, suggests either that recrudescence occurs independently of T-cell-mediated immunity or that it occurs because of a local impairment of T-cell function. Diminution of T-cell function could arise because of the local production of regulatory cytokines, activation-induced cell death, or exhaustion or through the action of regulatory T cells. What appears to be clear is that in both resistant and susceptible mice, immunity ultimately fails and the mice succumb to disease.

Protection induced by vaccination or afforded by memory immunity is frequently measured by determining the pulmonary bacterial burden within the first month after *M. tuberculosis* challenge; fewer studies measure survival (4, 15, 19, 25, 30). Our results show a discrepancy between lung CFU 21 days postchallenge and survival. Several explanations can be advanced to explain this disparity. One possibility is that the enhanced protection observed on day 21 postchallenge was due to the recent activation of innate immunity by the pathogen following primary infection. Another possibility is that the memory-immune response initially provides protection, but the primary response to the pathogen is able to "catch up". This possibility is supported by experiments showing that T cells obtained 20 days after infection of previously naïve or memory-immune mice have a similar capacity to transfer protection (21). While this is true in an adoptive transfer model, if bacterial replication is controlled earlier in memory-immune mice, the set point for the plateau phase will be lower and the survival would be predicted to be longer (19). Finally, the memory-immune response might fail late during the course of infection. As discussed above, the failure of a protective host response may be due to local factors such as the suppression of T-cell function.

In contrast with our results, other studies have shown that *Mycobacterium bovis* BCG vaccination has the capacity to prolong the survival of susceptible DBA/2 and resistant B6D2F1 and BALB/c mice (15, 19). Importantly, the BCG-vaccinated mice in these experiments were treated with antibiotics to clear BCG before challenge with *M. tuberculosis*. These studies differ from ours in a number of details that may have affected the ultimate outcome of infection. For example, the BCG-infected mice received antibiotics for 10 days and were challenged 3 days later. In our study, treatment extended for 60 days and the mice were challenged 30 days later. Although both antibiotic regimens appear to be efficacious at eliminating the bacteria, the status of mycobacterium-specific memory T cells may be very different. Another variable is that DBA/2 and BALB/c mice differ at the *nramp1* locus. Thus, while BALB/c mice are resistant to *M. tuberculosis*, their ability to clear BCG may be impaired compared to mouse strains that have the *nramp1*^{Gly169} allele, which is associated with resistance to intracellular infection (e.g., C3H, DBA/2) (8, 16, 17). Although this question has never been addressed directly, data showing that BCG Montreal can elicit protective immunity to *M. tuberculosis* irrespective of the *nramp1* genotype suggest that this difference is unlikely to be relevant (15, 23).

While the ultimate outcome of our experiments differs from those done by North (15, 19), they are nevertheless consistent with his assertion that vaccine-induced protection is manifested predominantly during the early phase of infection. While active *M. tuberculosis* infection may interfere with the

function of the memory-immune response, another important related question is whether bacterial persistence is required to maintain an optimum protective-immune response. Although this has not been definitively evaluated, there are a few studies that address this issue. T cells from rodents treated with antibiotics to clear BCG had a decreased ability to transfer resistance compared to untreated vaccinated mice (12, 24). Although BCG is considered avirulent and mice have been thought to clear BCG infection, it is now recognized that BCG is able to persist in mice for over a year depending on the dose and the route of administration (8, 24, 25). Thus, it is important to understand whether the ability of BCG to stimulate long-lived immunity is related to its ability to establish a persistent infection of the host.

It is surprising given the large number of BCG-vaccinated persons that few data exist addressing whether BCG persists following vaccination and whether persistence plays a role in maintaining its protective efficacy. Anecdotal reports of BCG persisting for years in vaccinated persons and in patients with bladder cancer following intravesical BCG therapy have been noted in the literature (1, 7, 35). Understanding whether the persistence of vaccine strains affects host immunity has important implications for the design of immunization strategies. For example, auxotrophic mutants of *M. tuberculosis* have excellent safety profiles, as they cannot persist even in immunocompromised hosts (28). On the other hand, in immunocompetent hosts, these mutants may be eliminated so rapidly by the innate immune system that a sustained protective-immune response may not be efficiently induced. Experimental data suggest that this may be more than a theoretical problem. Antibiotic treatment of mice infected with *Listeria monocytogenes* and BCG leads to the abrogation of T-cell-mediated immunity (5, 20). Antibiotic-mediated clearance of BCG results not only in a decreased antigen-specific T-cell response but also in impaired host protection (20). While experimental models have delineated how the primary immune response controls bacterial replication, understanding why recrudescence occurs has been much more difficult. It is well established that the impairment of cell-mediated immunity leads to an increased risk of reactivation tuberculosis. Understanding why immunity fails in experimental animals may provide insight into the basis for reactivation tuberculosis in people.

ACKNOWLEDGMENTS

This work was supported by National Institutes of Health grant R01 HL645450 and an American Lung Association grant Career Investigator Award to S.M.B.

We thank Chad Taylor and Jen Alt for their technical assistance.

REFERENCES

1. **Armbruster, C., W. Junker, N. Vetter, and G. Jaksch.** 1990. Disseminated bacille Calmette-Guerin infection in an AIDS patient 30 years after BCG vaccination. J. Infect. Dis. **162:**1216.
2. **Chackerian, A. A., J. M. Alt, T. V. Perera, C. C. Dascher, and S. M. Behar.** 2002. Dissemination of *Mycobacterium tuberculosis* is influenced by host factors and precedes the initiation of T-cell immunity. Infect. Immun. **70:** 4501–4509.
3. **Chackerian, A. A., T. V. Perera, and S. M. Behar.** 2001. Gamma interferon-producing $CD4^+$ T lymphocytes in the lung correlate with resistance to infection with *Mycobacterium tuberculosis*. Infect. Immun. **69:**2666–2674.
4. **Cooper, A. M., J. E. Callahan, M. Keen, J. T. Belisle, and I. M. Orme.** 1997. Expression of memory immunity in the lung following re-exposure to Mycobacterium tuberculosis. Tuber. Lung Dis. **78:**67–73.
5. **Feng, C. G., C. M. Collazo-Custodio, M. Eckhaus, S. Hieny, Y. Belkaid, K. Elkins, D. Jankovic, G. A. Taylor, and A. Sher.** 2004. Mice deficient in LRG-47 display increased susceptibility to mycobacterial infection associated with the induction of lymphopenia. J. Immunol. **172:**1163–1168.
6. **Flynn, J. L., and J. Chan.** 2001. Immunology of tuberculosis. Annu. Rev. Immunol. **19:**93–129.
7. **Gonzalez, O. Y., D. M. Musher, I. Brar, S. Furgeson, M. R. Boktour, E. J. Septimus, R. J. Hamill, and E. A. Graviss.** 2003. Spectrum of bacille Calmette-Guerin (BCG) infection after intravesical BCG immunotherapy. Clin. Infect. Dis. **36:**140–148.
8. **Gros, P., E. Skamene, and A. Forget.** 1981. Genetic control of natural resistance to Mycobacterium bovis (BCG) in mice. J. Immunol. **127:**2417–2421.
9. **Kamath, A. B., J. Alt, H. Debbabi, and S. M. Behar.** 2003. Toll-like receptor 4-defective C3H/HeJ mice are not more susceptible than other C3H substrains to infection with *Mycobacterium tuberculosis*. Infect. Immun. **71:**4112–4118.
10. **Kamath, A. B., J. Alt, H. Debbabi, C. Taylor, and S. M. Behar.** 2004. The major histocompatibility complex haplotype affects T-cell recognition of mycobacterial antigens but not resistance to *Mycobacterium tuberculosis* in C3H mice. Infect. Immun. **72:**6790–6798.
11. **Kaufmann, S. H.** 2001. How can immunology contribute to the control of tuberculosis? Nat. Rev. Immunol. **1:**20–30.
12. **Lefford, M. J., and D. D. McGregor.** 1974. Immunological memory in tuberculosis. I. Influence of persisting viable organisms. Cell Immunol. **14:**417–428.
13. **Masopust, D., V. Vezys, A. L. Marzo, and L. Lefrancois.** 2001. Preferential localization of effector memory cells in nonlymphoid tissue. Science **291:** 2413–2417.
14. **Medina, E., and R. J. North.** 1998. Resistance ranking of some common inbred mouse strains to Mycobacterium tuberculosis and relationship to major histocompatibility complex haplotype and Nramp1 genotype. Immunology **93:**270–274.
15. **Medina, E., and R. J. North.** 1999. Genetically susceptible mice remain proportionally more susceptible to tuberculosis after vaccination. Immunology **96:**16–21.
16. **Medina, E., and R. J. North.** 1996. Evidence inconsistent with a role for the Bcg gene (Nramp1) in resistance of mice to infection with virulent Mycobacterium tuberculosis. J. Exp. Med. **183:**1045–1051.
17. **Medina, E., and R. J. North.** 1996. Mice that carry the resistance allele of the Bcg gene (Bcgr) develop a superior capacity to stabilize bacille Calmette-Guerin (BCG) infection in their lungs and spleen over a protracted period in the absence of specific immunity. Clin. Exp. Immunol. **104:**44–47.
18. **Nicolle, D., C. Fremond, X. Pichon, A. Bouchot, I. Maillet, B. Ryffel, and V. J. F. Quesniaux.** 2004. Long-term control of *Mycobacterium bovis* BCG infection in the absence of Toll-like receptors (TLRs): investigation of TLR2-, TLR6-, or TLR2-TLR4-deficient mice. Infect. Immun. **72:**6994–7004.
19. **North, R. J., R. LaCourse, and L. Ryan.** 1999. Vaccinated mice remain more susceptible to *Mycobacterium tuberculosis* infection initiated via the respiratory route than via the intravenous route. Infect. Immun. **67:**2010–2012.
20. **Olsen, A. W., L. Brandt, E. M. Agger, L. A. van Pinxteren, and P. Andersen.** 2004. The influence of remaining live BCG organisms in vaccinated mice on the maintenance of immunity to tuberculosis. Scand. J. Immunol. **60:**273–277.
21. **Orme, I. M.** 1988. Characteristics and specificity of acquired immunologic memory to Mycobacterium tuberculosis infection. J. Immunol. **140:**3589–3593.
22. **Orme, I. M.** 1987. The kinetics of emergence and loss of mediator T lymphocytes acquired in response to infection with Mycobacterium tuberculosis. J. Immunol. **138:**293–298.
23. **Orme, I. M., and F. M. Collins.** 1984. Demonstration of acquired resistance in Bcgr inbred mouse strains infected with a low dose of BCG montreal. Clin. Exp. Immunol. **56:**81–88.
24. **Orme, I. M., and F. M. Collins.** 1986. Aerogenic vaccination of mice with Mycobacterium bovis BCG. Tubercle **67:**133–140.
25. **Palendira, U., A. G. D. Bean, C. G. Feng, and W. J. Britton.** 2002. Lymphocyte recruitment and protective efficacy against pulmonary mycobacterial infection are independent of the route of prior *Mycobacterium bovis* BCG immunization. Infect. Immun. **70:**1410–1416.
26. **Pope, C., S. K. Kim, A. Marzo, D. Masopust, K. Williams, J. Jiang, H. Shen, and L. Lefrancois.** 2001. Organ-specific regulation of the CD8 T cell response to Listeria monocytogenes infection. J. Immunol. **166:**3402–3409.
27. **Sallusto, F., J. Geginat, and A. Lanzavecchia.** 2004. Central memory and effector memory T cell subsets: function, generation, and maintenance. Annu. Rev. Immunol. **22:**745–763.
28. **Sambandamurthy, V. K., X. Wang, B. Chen, R. G. Russell, S. Derrick, F. M. Collins, S. L. Morris, and W. R. Jacobs, Jr.** 2002. A pantothenate auxotroph of Mycobacterium tuberculosis is highly attenuated and protects mice against tuberculosis. Nat. Med. **8:**1171–1174.
29. **Scanga, C. A., V. P. Mohan, H. Joseph, K. Yu, J. Chan, and J. L. Flynn.** 1999. Reactivation of latent tuberculosis: variations on the Cornell murine model. Infect. Immun. **67:**4531–4538.
30. **Serbina, N. V., and J. L. Flynn.** 2001. $CD8^+$ T cells participate in the memory immune response to *Mycobacterium tuberculosis*. Infect. Immun. **69:**4320–4328.

31. **Smith, P. G. and A. R. Moss.** 1994. Epidemiology of tuberculosis, p. 47–60. *In* B. R. Bloom (ed.), Tuberculosis: pathogenesis, protection, and control. American Society for Microbiology, Washington, D.C.
32. **Turner, J., M. Gonzalez-Juarrero, B. M. Saunders, J. V. Brooks, P. Marietta, D. L. Ellis, A. A. Frank, A. M. Cooper, and I. M. Orme.** 2001. Immunological basis for reactivation of tuberculosis in mice. Infect. Immun. **69:**3264–3270.
33. **Wherry, E. J., and R. Ahmed.** 2004. Memory CD8 T-cell differentiation during viral infection. J. Virol. **78:**5535–5545.
34. **Zaph, C., J. Uzonna, S. M. Beverley, and P. Scott.** 2004. Central memory T cells mediate long-term immunity to Leishmania major in the absence of persistent parasites. Nat. Med. **10:**1104–1110.
35. **Zeyland, J., and E. Piasecka-Zeyland.** 1936. Sur la vitalité du BCG dans l'organisme vacciné. Ann. Inst. Pasteur **56:**46–51.

Editor: J. L. Flynn